Available online at www.sciencedirect.com
ScienceDirect
Catalysis Today 120 (2007) 262–269
CATALYSIS TODAY
www.elsevier.com/locate/cattod

Enhanced hydrogen sorption kinetics of magnesium by destabilized $MgH_{2-\delta}$

A. Borgschulte *, U. Bösenberg, G. Barkhordarian, M. Dornheim, R. Bormann

GKSS-Research Center Geesthacht GmbH, Institute for Materials Research, Max-Planck-Strasse 1, 21502 Geesthacht, Germany

Available online 13 November 2006

Abstract

The kinetics of the reversible reaction of hydrogen gas with magnesium forming MgH_2 is enhanced significantly by the addition of transition metals oxide catalysts and by using nanostructured powders. Hydrogen absorption and desorption properties of such systems were studied by differential scanning calorimetry (DSC) under hydrogen atmosphere, from which the heat of hydride formation and decomposition is determined. Apart from Mg and stoichiometric MgH_2, we find an additional, slightly destabilized phase, which is formed prior to MgH_2 upon hydrogenation. The amount of this phase depends on the degree of nanostructuring and the used additive. X-ray diffraction measurements confirm the compared to MgH_2 slightly different lattice parameters of the intermediate phase. The results correspond to recent neutron diffraction measurements, by which a new $MgH_{2-\delta}$ phase was found. We propose that this destabilized phase acts as a gateway for de-hydrogenation of MgH_2.

Keywords: Catalyzed MgH_2; Oxide; Hydrogen sorption kinetics; Intermediate phase; DSC; XRD

1. Introduction

Hydrogen is the ideal means of storage, transport and conversion of energy for a comprehensive clean-energy concept [1]. Regarding the use of hydrogen as fuel for the zero-emission vehicle, the main problem is the storage of hydrogen. Metal hydrides offer a safe alternative to storage in compressed or liquid form. In addition, metal hydrides have the highest storage capacity by volume. Mg hydride has also a high storage capacity by weight and is therefore favored for mobile applications. However, due to the slow kinetics and the high stability, Mg is not suitable for application in hydrogen storage systems. In recent years, significant progress has been made using nanocrystalline Mg produced by high energy milling [2] and adding suitable catalysts. [3–5] For technical application, sufficiently fast kinetics has been achieved at 300 °C [4].

Still, the exact phase of the additive, its role and the corresponding mechanisms remained unclear, which led to a controversial debate on the origin of the effects. In particular, Huot et al. report a catalytic effect of transition elements like Nb and Ta in bulk (nanocrystalline) Mg hydrides and explain their catalytic effect by the formation of a metastable niobium (tantalum) hydride phase which acts as a gateway through which hydrogen released from MgH_2 is flowing [3]. Surprisingly, transition metal oxides have shown remarkably higher effects than the pure metals [4]. By an analysis of the desorption kinetics the authors try to evaluate the critical kinetic step of the reactions in different temperatures and catalyst contents. They conclude that oxide catalysts lower the surface barrier during desorption [6]. Interestingly, a similar result (i.e. a first order reaction with surface constraint) has been also found by Hanada et al. for pure 3d-elements as catalysts [5]. In this study, nanocrystalline Ni was found to have highest catalytic activity. Clean surfaces of 3d-elements, in particular Ni, are well known for their catalytic activity for hydrogen dissociation [7]. Their activity is orders of magnitude higher than that of the transition metal oxides used by Barkhordarian et al. [6], while these oxides are the better additives for hydrogen uptake [8]. Moreover, (surface-) oxidation of Ni does not alter drastically its catalytic properties for hydrogen absorption [9] - in contrast to Nb, where a strong dependency on the oxygen content was found [4,10]. These inconsistencies are hints that hydrogen uptake hinge on the details of complex kinetic phenomena.

* Corresponding author. Present address: Empa, Swiss Federal Laboratories for Materials Testing and Research, Laboratory for Hydrogen & Energy, Überlandstrasse 129, CH-8600 Dübendorf, Switzerland.
Tel.: +41 44 823 4639; fax: +41 44 821 6244.
E-mail address: andreas.borgschulte@empa.ch (A. Borgschulte).

0920-5861/$ – see front matter © 2006 Elsevier B.V. All rights reserved.
doi:10.1016/j.cattod.2006.09.031

Generally, the effect of surface catalysts on the sorption properties of Mg is unexpected. Hydrogen absorption of bulk magnesium is controlled by the diffusion through MgH_2 [11,12]. The diffusional properties of hydrogen in magnesium have been investigated by Renner and Grabke, who determined a diffusion coefficient of $D = 4.0 \times 10^{-13}$ m^2/s at 300 K [13]. Using neutron scattering, Töpler et al. found H-diffusion in MgH_2 to be three orders of magnitude lower than in Mg (at 350 K) [14]. By XPS, Spatz et al. have determined that the overall hydrogen diffusion coefficient for the Mg-to-MgH_2-transition (including nucleation and growth) is as low as $D = 1.1 \times 10^{-20}$ m^2/s [15]. The effect of this kinetic constraint can be diminished using Mg nano-particles (grains) [11]. However, because relatively high temperatures have to be used, the grains coarsen and their size after cycling increase from initially 10 nm to 80 nm (130 nm) according to Ref. [4] (Ref. [16]). This is actually too large to reduce the diffusion-time significantly [11].

A most recent publication reports on a new sub-stoichiometric $MgH_{2-\delta}$-phase in ball-milled MgH_2 [16]. Sub-stoichiometric hydrides are known to have better diffusional properties than saturated hydrides [17]. We will demonstrate in this publication that the aforementioned enhanced kinetics is correlated to this phase, which is only formed in ball-milled samples and here prominently in oxide-catalyzed systems. We measure the thermodynamic properties of it and prove its existence by X-ray diffraction. Sub-stoichiometric magnesium hydride is slightly less stable than MgH_2, but kinetically favored. Therefore this phase acts as a gateway through which hydrogen released from MgH_2 is flowing. Furthermore, the amount of this phase can be correlated to the used catalyst and preparation method. The experimental results are summarized in a model, which opens a new view on the working of hydrogen uptake catalysts.

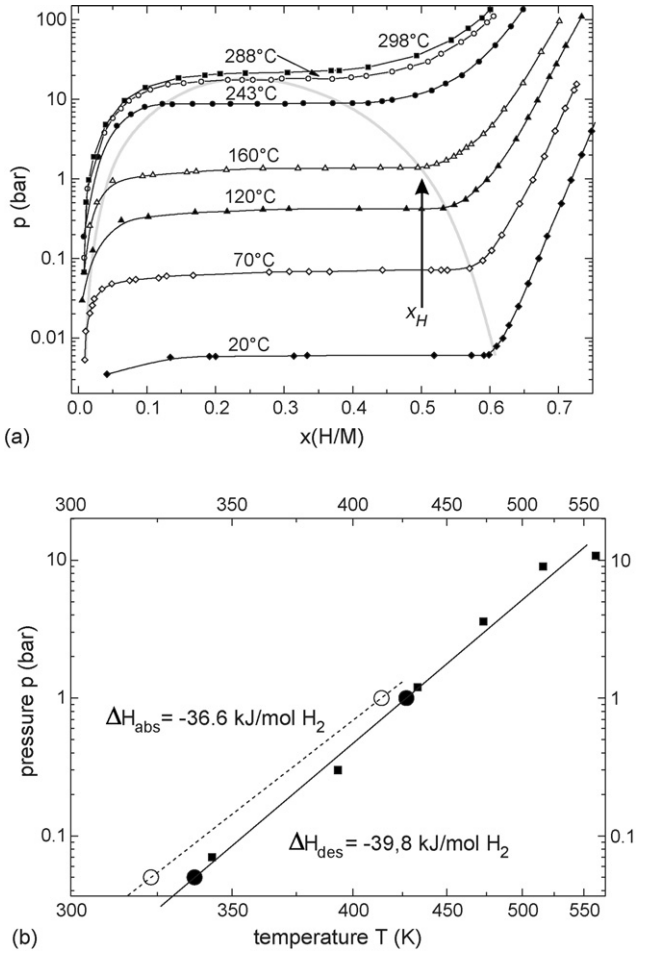

Fig. 1. (a) *pcT*-diagram of Pd–H, as measured by Frieske and Wicke [20]. The grey line indicates the binodal curve. (b) van't Hoff plot of Pd–H constructed form equilibrium pressures obtained by *pcT*-curves from (a) and DSC-measurements, respectively.

2. Experimental

Thermodynamic and kinetic characterization is performed by isobaric DSC measurements. These measurements provide thermodynamic data such as reaction enthalpy, miscibility gap width and pressure-temperature relation, and kinetic data such as activation energy and hysteresis [18]. For these measurements, a Perkin Elmer DSC 7 is used under 1 bar of pure H_2 and Ar/H_2 mixtures, respectively. The process gas (5 N) is purified directly before entering the DSC using an oxygen getter (Messer-Griesheim oxysorb). The hydride sample (typically 10 mg) is held in an aluminum pan located in a double-furnace system for DSC measurements. A second aluminum pan is used as a reference.

As the usage of DSC measurements for the measurement of pressure-temperature relations is not very common, we present as an example the measurement of the archetypical Pd–H system. Fig. 1(a) shows the *pcT* diagram of Pd–H as measured by Frieske and Wicke [20]. Outside the miscibility gap there is a slight change of the hydrogen content dependent on the temperature. This means for isobaric DSC measurements that the heat flow *j* involved will not be sufficient for detection. Only when achieving the miscibility gap, the hydrogen content will change rapidly ($x_H(\alpha) \Rightarrow x_H(\beta)$) so that the integrated DSC signal $\Delta Q_{abs,des} = \int j/r\,dt$ with r being the heating rate will result in accordance with the enthalpy change

$$\Delta Q_{abs,des} = \Delta H_{abs,des} \cdot x_H, \quad (1)$$

where $\Delta Q_{abs,des}$ is the molar heat of hydride formation. Because the miscibility gap (i.e. the amount of exchanged hydrogen x_H) decreases with rising pressure, the measured enthalpy change will decrease in this direction.

Fig. 2 shows corresponding isobaric DSC-measurements of Pd at p_{H2} = 1 bar. The integrated DSC signal is nearly identical independent of the heating rate, confirming that in all cycles the same amount of hydrogen is exchanged. The onset temperatures $T_{abs,des}$ are obtained as secondary information from the isobaric DSC measurements (see Fig. 1). The *p–c–T* relations connect these temperatures to the applied pressure via the van't Hoff equation

$$\ln p = \frac{2\Delta H_{abs,des}}{RT_{abs,des}} - \frac{2\Delta S}{R}, \quad (2)$$

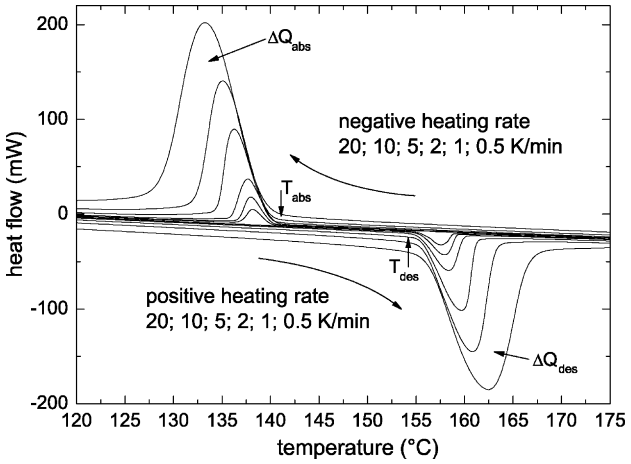

Fig. 2. Isobaric DSC-measurements (p = 1 bar hydrogen) of the desorption and absorption of hydrogen in Pd at various heating (cooling) rates.

where $\Delta H_{abs,des}$ and the entropy of hydride formation/decomposition ΔS refer to 1 mol H_2. Fig. 1(b) represents the van't Hoff-plot of Pd–H as obtained by *pcT*-curves (from Frieske and Wicke [20]) and by isobaric DSC, respectively. The difference between the values of heat absorption/desorption derived via van't Hoff equation $\Delta H_{abs,des}$ and those directly measured from the enthalpy change can be explained by the known phenomenon of hysteresis. The directly measured values do not display a difference (ΔQ_{abs} = 18.8 kJ/mol PdH_x, ΔQ_{des} = −18.2 kJ/mol PdH_x), as the initial and final stages for absorption and desorption are identical, but exchanged. However, for the nucleation of a new phase (β for absorption, α for desorption) a thermodynamic overpotential is needed. Thus, the plateau pressures or the onset temperatures at isobaric conditions, respectively, differ and so do the corresponding heats of hydride formation (ΔH_{abs} = 36.6 kJ/mol H_2, ΔH_{des} = 39.8 kJ/mol H_2). The exchanged amount of hydrogen is calculated by Eq. (1). The resulting value is in good agreement with known values ($x_{H,DSC}$ = 0.5, to be compared with x_H (p = 1 bar) = 0.52, see Fig. 1), taking into account the considerable experimental uncertainties in the determination of the binodal curve.

Pure magnesium hydride (95 mass% MgH_2, 5 mass% Mg) was provided by Th. Goldschmidt AG. The average particle size was 200 μm as reported by the manufacturer. Milling was carried out with a Fritsch P5 planetary mill in a stainless steel vial and a ball to powder weight ratio of 10:1. Initial milling time was 20 h. At regular intervals, the powder was slackened. Afterwards, 0.5 mol% Nb_2O_5, Fe_3O_4 and ZrO_2, respectively, was added (99.91 metal), and milled for further 20 h. All handling of the powders, including milling and measurements, was performed inside glove boxes under a continuously purified Ar atmosphere (oxygen and water content around 1 ppm). It is worth mentioning that the amount of oxygen in the samples increases after ball-milling even without adding oxides. The increase of oxygen during milling is due to the high reactivity of magnesium. Because the reduction potential of Mg is very low, the small fraction (5 mass%) of pure magnesium, which is present in the starting powder can easily reduce oxides attached to the vial and balls and form MgO [2].

Structural analyses were carried out at room temperature using a X-ray diffractometer (Bruker D5000 with Cu Kα radiation, equipped with a secondary monochromator. X-ray sample holders were filled inside the glove box and covered with a Kapton foil to minimize oxidation during the X-ray measurement.

3. Results

Fig. 3 shows the corresponding first desorption measurements of as prepared samples in 50.065 mbar hydrogen. The desorption maxima of the first desorption of ball-milled and catalyzed MgH_2 materials are indeed shifted towards lower temperatures compared to conventional MgH_2, in good agreement with literature data [3,4]. This is usually taken as evidence for a faster kinetics, which is indeed plausible by comparing the desorption temperatures with desorption kinetics measured by a Sieverts apparatus at constant T = 300 °C (see Fig. 4, taken from Ref. [6]). At the maximum, the system has highest desorption rate. The lower this temperature, the smaller is the chemical overpotential needed to reach this maximum rate. However, the various peak structures observed in different systems complicate the characterization of the desorption kinetics by only one temperature parameter. It is worth to mention that the broadening and sometimes even splitting of the desorption peaks was reported earlier [2], while its origin remained unclear. It can be suggested, though, that several intermediate steps with different kinetic characteristics are involved in the desorption process.

From a thermodynamic point of view, the onset temperatures are the important parameter, though (compare Section 2). Apart from pure MgH_2, the onset temperatures seem to be identical — independent of the used catalyst. This is evidence that the catalysts do not change the thermodynamic properties of MgH_2. Furthermore, the onset temperatures of the first desorption fit

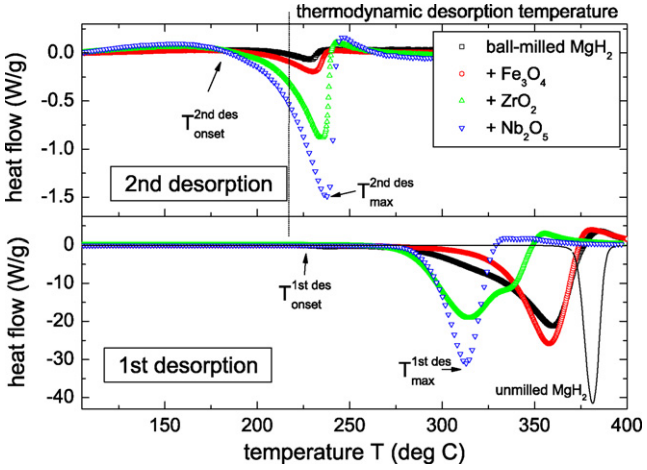

Fig. 3. DSC-traces in Ar–5% H_2-atmosphere of non ball-milled MgH_2 and ball-milled MgH_2 with various catalysts. Heating rate is 10 K/min. The bottom graph represents the desorption behavior of as-prepared samples. The top graph displays the DSC-measurements after partial reabsorption of hydrogen during cooling in Ar–5% H_2-atmosphere at 10 K/min. The indicated thermodynamic desorption temperature is calculated from literature data [21].

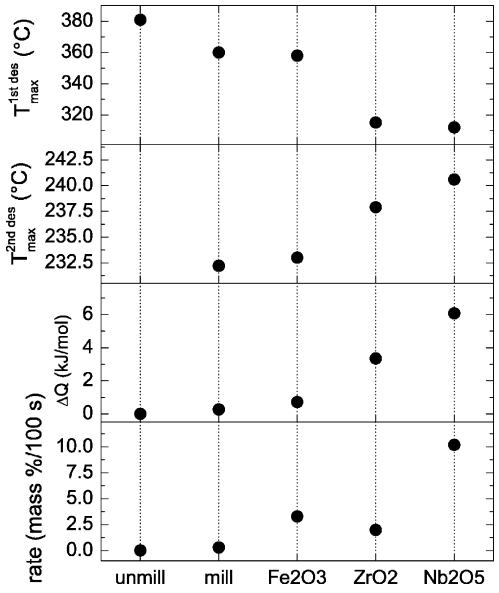

Fig. 4. The graph compares the temperature maxima of the first and the second desorption, respectively, and the corresponding desorbed heats ΔQ as obtained from Fig. 3 for various catalyzed, ball-milled MgH_2 samples with the averaged desorption rates, measured by a Sieverts apparatus at constant $T = 300$ °C (from Ref. [4]).

reasonable well with the thermodynamic (equilibrium) desorption temperature T_{des}, calculated from literature data [21].

Consecutively, the absorption was performed during cooling 10 K/min, which is too fast to guarantee a full loading of the Mg. Still, a small amount of hydrogen is absorbed, which is measured during the 2nd desorption. This 2nd desorption shows a completely different behavior than expected from the 1st one. The onset temperatures are drastically lowered compared with the initial desorption. Moreover, the desorption maxima and onset temperatures are nearly identical for all investigated systems within 10 K. An important fact is that the enthalpy change varies with the used catalyst. This is shown in more detail in Fig. 4. Maximum absorbed heat is 6 kJ/mol. This value corresponds to a reacted fraction of 8% reference to MgH_2. Interestingly, the amount of reabsorbed hydrogen roughly scales with desorption rates at constant temperature $T = 300$ °C, as measured by a Sieverts apparatus (from Ref. [6], see Fig. 4). Non-ball milled MgH_2 does not show any reabsorption under these conditions, and in almost the same manner behaves the sorption in a Sieverts apparatus.

The amount of reabsorbed hydrogen can originate from two mechanisms: the hydrogen uptake kinetics varies or the feasibility to form this particular state controls the reabsorption. However, the relation between the desorption maxima and the amount of reabsorbed hydrogen advises, that the desorption kinetics is roughly the same for all systems, while the only amount of the phase is changed (Fig. 4). This suggests that the reabsorption is controlled by the feasibility of forming an intermediate phase. On the other hand, the overall hydrogen sorption kinetics does change. This can only be explained, if this intermediate state is a kind of kinetically favored, but thermodynamically less stable state, before the final MgH_2 is formed.

To clarify, whether the decrease of the onset temperatures has its origin in thermodynamics or kinetics, we study desorption and absorption cycles with various rates of the sample, i.e. the heating and cooling of the samples in Ar–5% H_2 and pure H_2 atmosphere, respectively (Fig. 5). As described in the experimental section, the onset temperatures determine the thermodynamic absorption and desorption temperatures, respectively. Interestingly, desorption and absorption temperatures are identical for fast heating and cooling rates. This may be interpreted as a hysteresis-free hydrogen sorption, which is in disagreement with literature as the Mg–MgH_2-system is known for its large hysteresis [4]. A first idea gives the small intensity of the signals. Assuming a constant heat of hydride formation, only around 8% of the Mg has reacted to MgH_2 (at $p_{H2} = 50$ mbar and a cooling rate of 10 K/min, see also Fig. 4). That means that only a small part of the total amount

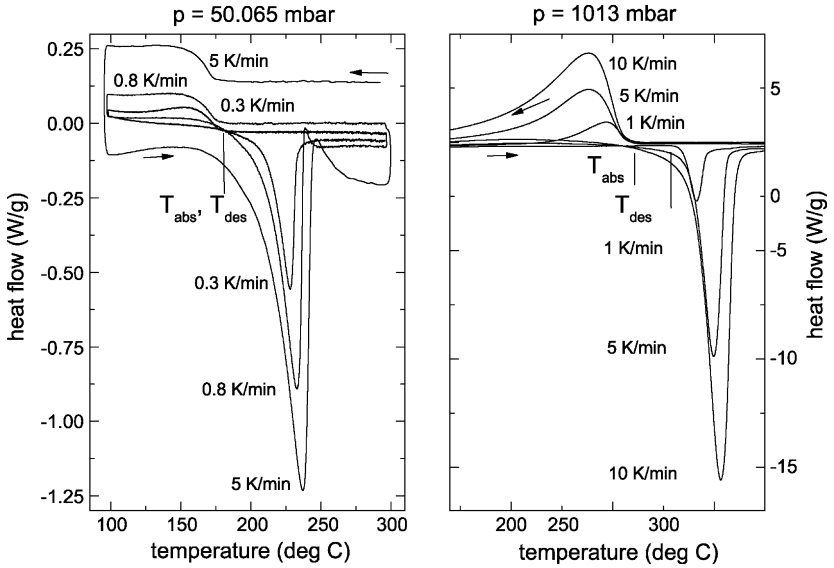

Fig. 5. DSC-traces in H_2- and Ar–5% H_2-atmosphere (corresponding to 1013 mbar and 50.065 mbar hydrogen), respectively, of Nb_2O_5-catalyzed MgH_2 at various heating (cooling) rates. The peak onset during heating and cooling defines the desorption and absorption temperature, respectively.

of Mg is capable of taking up hydrogen under these conditions. Accordingly, the main part of the Mg is kinetically much slower and therefore responsible for the large hysteresis measured under equilibrium conditions (e.g. Ref. [2]). Furthermore, the onset temperatures as deduced by the DSC-traces in Fig. 5 seem to depend on the kinetics. This also underlines the existence of a small, kinetically more favored but thermodynamically less stable phase than that of the equilibrium MgH_2 phase.

As changing the kinetics also alters the resolution of the spectrometer, the desorption is performed at the same conditions (in particular the same heating rate), while the amount of initially absorbed hydrogen is varied by a modified absorption process. This is shown in Fig. 6. After the initial (first) desorption, curve (a) is loaded during cooling with 5 K/min, while the absorption in (b) is supported by keeping the sample at constant $T = 160\ ^\circ C$ for 100 min and subsequent cooling with 5 K/min. Thereby more hydrogen is absorbed and, additionally, the system can relax better towards thermodynamic equilibrium.

The subsequent desorption with equal heating rate for both curves reveals indeed a larger peak and therefore higher amount of hydrogen for curve (b). The enthalpy change is around 31 kJ/mol and 33 kJ/mol for curve (a) and (b), respectively. These values correspond to a reacted fraction of 50% reference to MgH_2 and is in accordance with the reacted fraction reported for similar conditions in Ref. [19]. Surprisingly, though, is the shift of the onset by nearly 10 K. Furthermore, the curve shape and the desorption maximum have changed from (a) to (b). The sample after phase (a) proceeds absorbing hydrogen also during heating. At a certain temperature, which we define as the 'kinetic' desorption temperature, desorption starts immediately without hysteresis. The sample does not absorb hydrogen during heating in measurable amount after phase (b) and a continuous transition towards desorption is not observed. The corresponding hysteresis is then the difference between absorption temperature and equilibrium desorption temperature. Accordingly, the desorption temperature is now shifted to higher temperatures.

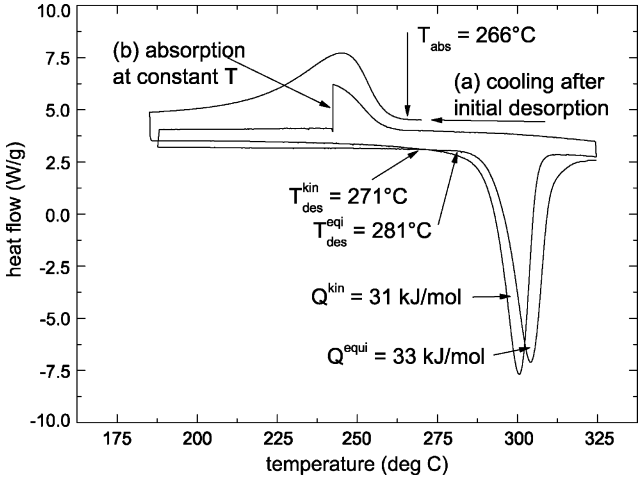

Fig. 6. Determination of the equilibrium desorption temperature. After the initial desorption, curve (a) is loaded during cooling with 5 K/min, while the absorption in (b) is supported by keeping the sample at constant $T = 160\ ^\circ C$ for 100 min. The subsequent desorption is performed with a heating rate of 5 K/mol for both curves. For better visibility, the absorption curves have been shifted.

Assuming the onset temperatures being the thermodynamic minimum (maximum) temperature for desorption (absorption), the DSC-measurements can be summarized in a van't Hoff plot (Fig. 7). The pressure dependency on temperature is correlated with the stability of the corresponding phase (see Section 2). The equilibrium desorption temperature is derived from DSC-traces with 0.6 K/min after full absorption in 1 bar hydrogen and the 'kinetic' desorption temperatures from DSC-traces with 5 K/min after dynamical absorption.

We obtain $\Delta H_{abs} = -69\ kJ/mol\ H_2$ for absorption, and $\Delta H^{kin}_{des} = -64\ kJ/mol\ H_2$ and $\Delta H^{equi}_{des} = -75\ kJ/mol\ H_2$ for desorption, determined by the two different experimental conditions, respectively. The equilibrium heat of desorption $\Delta H^{equi}_{des} = -75\ kJ/mol\ H_2$ and the corresponding entropy of $\Delta S^{equi}_{des} = 136\ kJ/(K\ mol\ H_2)$ is in perfect agreement with literature data [21].

We conclude that two phases are formed during hydrogenation of Mg: a slightly less stable but kinetically favored phase and a more stable, but kinetically constraint one. The first phase is the intermediate step, probably non-stoichiometric $MgH_{2-\delta}$, before the more stable, stoichiometric MgH_2-phase (i.e. the equilibrium phase) is formed.

This corresponds to recent neutron diffraction measurements, by which a new $MgH_{1.2}$ phase in ball-milled, Nb-catalyzed MgH_2 was found [16]. The authors found an increase in the unit cell volume of Mg during loading, from which they estimated a temperature rise of around 12 K, expecting a higher equilibrium pressure – which is in perfect agreement with the van't Hoff plot presented in Fig. 7.

To undoubtedly attribute the measured heat of formations to those particular phases, we performed X-ray diffraction on three representative samples: one after complete desorption and small absorbtion during cooling (similar to curve (a) in Fig. 6), a fully loaded sample and one intermediate step. Fig. 8 also shows the calculated X-ray patterns for stoichiometric and substoichiometric magnesium deuteride using the structure data by Schimmel et al. [16], see also Table 1. Unfortunately,

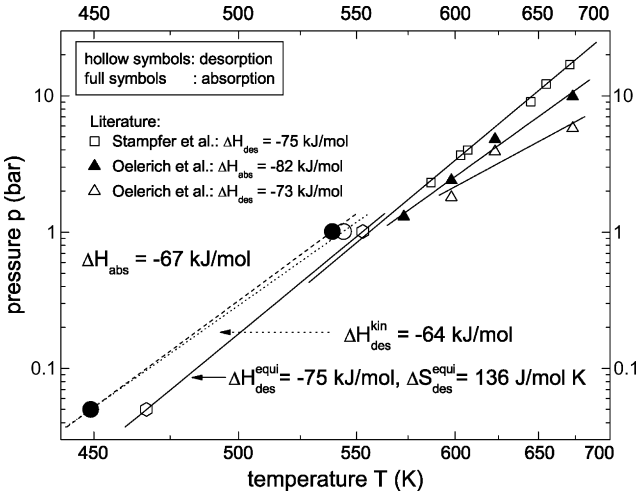

Fig. 7. Van't Hoff plot of Mg–H constructed form absorption and desorption temperature obtained by DSC-measurements. Literature is added for comparison: Stampfer et al. [21], Oelerich et al. [23].

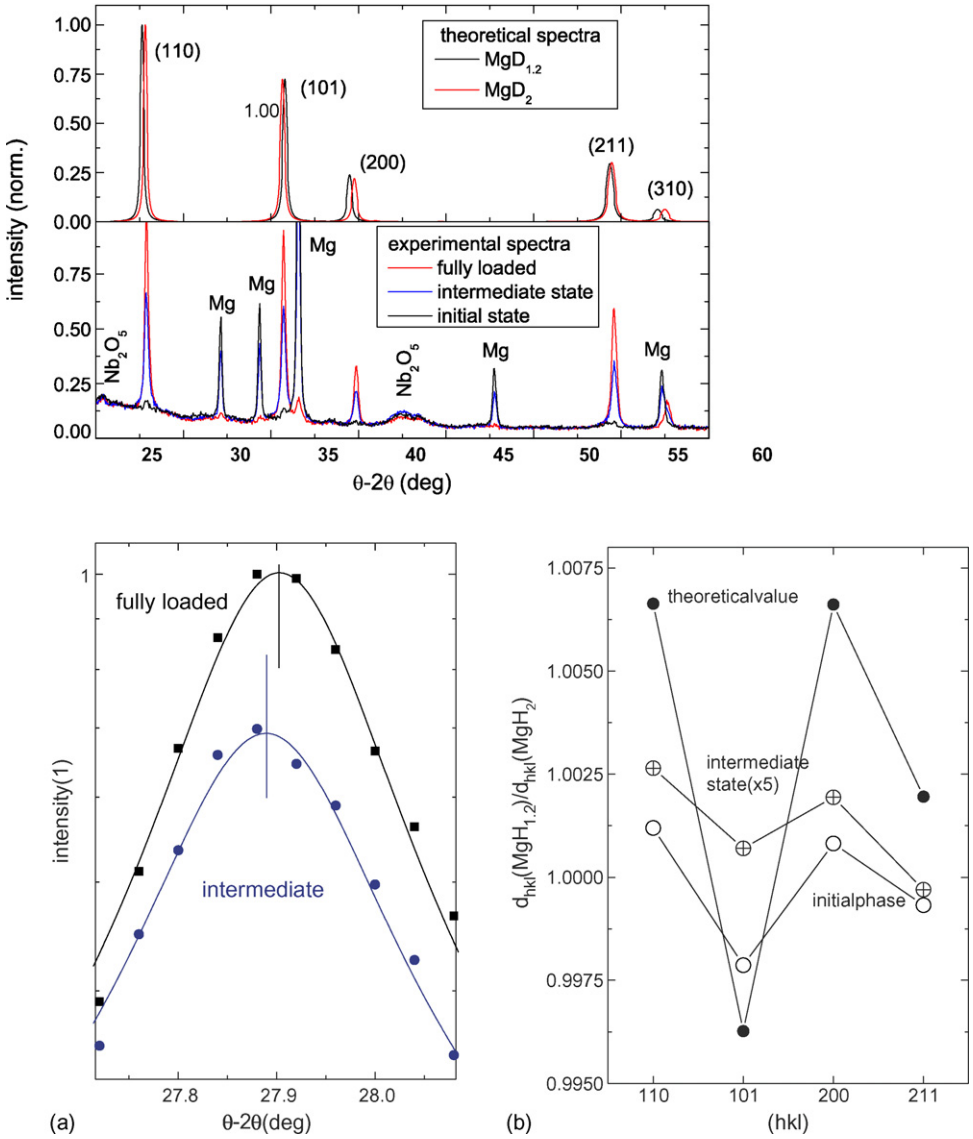

Fig. 8. Top: X-ray powder diffraction of nanocrystalline MgH_x at various hydrogenation states compared to simulated X-ray diffraction spectra of $MgH_{1.2}$ and MgH_2 using literature data (Ref. [16]). Bottom: (a) enlargement of the MgH_x (110) peaks and corresponding fits. (b) Ratio of the lattice spacings d_{hkl} of measured values and calculated $MgH_{1.2}$ and MgH_2.

Schimmel et al. measured deuterated samples at 300 °C, which have different lattice parameters than hydrogenated samples at room temperature. Yet, we presume that the relative shifts of the lattice spacings and the associated shifts of the X-ray peaks are preserved in hydrogenated samples. The change of the lattice parameters is relatively small (see Fig. 8(a)), so that experimental errors due to misalignment (powder samples) etc. might falsify the results. Thus we compare the ratio of the fitted X-ray peaks θ_{hkl}, which correspond to the ratio of the lattice spacings d_{hkl}:

$$r_{hkl} = \frac{d_{hkl}(\mathrm{MgH_2})}{d_{hkl}(\mathrm{MgH_{2-\delta}})} = \frac{\sin\theta_{hkl}(\mathrm{MgH_{2-\delta}})}{\sin\theta_{hkl}(\mathrm{MgH_2})}.$$

The measured ratios r_{hkl} are smaller than those of Schimmel et al. [16], but follow the same trend as anticipated by the calculation (see Fig. 8). This is a proof for the same lattice distortion of magnesium hydride and thus for the existence of substoichiometric $MgH_{2-\delta}$ as proposed in literature. Assuming the same crystal symmetry, we can calculate lattice parameter from our measurements, which are summarized in Table 1.

The slight disagreement between literature data and experiment of the lattice parameters of the intermediate state

Table 1
Lattice parameters of $MgH(D)_x$. Used space group $P4_2/mnm$ no. 136 (tetragonal) and atom positions according to Ref. [16]

Literature	a (Å)	c (Å)	Present paper	a (Å)	c (Å)
$MgD_{1.2}$	4.56	3.00	Initial MgH_x	4.529(7)	3.00(3)
			Intermediate MgH_x	4.524(4)	3.00(2)
MgD_2	4.530	3.025			
MgH_2	4.518	3.022	Fully loaded MgH_x	4.522(9)	3.00(6)

Literature values for deuterated samples from Ref. [16], for MgH_2 from Ref. [22].

can be explained by the two different isotopes (H and D) used and by the temperature difference. Furthermore, as the intermediate state is only kinetically favored but thermodynamically less stable than the final state d_{hkl}, the intermediate state will slowly transform into its final state. To circumvent this problem, *in-situ* measurements are planned.

4. Discussion

We start the discussion with a short summary of the results:

- A small fraction of Mg reacts with hydrogen without showing a significant hysteresis. This fraction only exists in ball-milled samples; its amount varies with the used catalyst.
- Further loading of Mg is kinetically hindered.
- From the desorption temperatures we estimated the stability of the fraction, which was found to be less stable than the equilibrium MgH_2.
- We attributed this fraction to the recently discovered substoichiometric magnesium dihydride and prove its existence by X-ray diffraction.

Together with literature data, we use these results to build a depictive model of the functioning of ball-milled magnesium hydride storage materials (Fig. 9). Ball-milling decreases the grain size of MgH_2 down to approximately 10 nm (Fig. 9(i) ⇒ (ii)) [24]. These nanoclusters coarsen during cycling and the grain size increases up to 80 nm to 130 nm, as estimated by the width of X-ray peaks in the present paper (Scherrer's-formula) and as reported by Schimmel et al. [16], respectively. During the initial stage of hydriding, the DSC-trace of an additional destabilized magnesium hydride phase is observed, which is attributed to substoichiometric $MgH_{2-\delta}$.

A non-answered question is the location of this phase. Is it a kind of intermediate state during sorption of the whole grain or is it MgH_2 at special places in the grain, e.g. at grain boundaries as sketched in Fig. 9? $MgH_{2-\delta}$ does only occur in ball-milled MgH_2 and, thus, might be a characteristic for small particles. Wagemans et al. indeed postulate the destabilization of small MgH_2 clusters for cluster sizes of less than 1.3 nm [25]. However, the measured crystal sizes are much larger. The estimated amount of the destabilized phase varies with the used catalysts, underlining the assumption of a grain boundary phase. It is known from similar metal–hydride systems (e.g. Gd–H [26], Zr–H [27]), that oxygen destabilizes the β phase and stabilizes the α phase (i.e. increases the solubility range of H in the metal). The solubility of oxygen in Mg is negligibly low, though [28]. We propose, that oxide interfaces attached to the oxide catalysts might locally destabilize the magnesium hydride phase. The presence of these (hydr-) oxide interfaces has been recently proven by XPS [29]. The strong interaction between Mg and oxide catalysts leads to the formation of a mixed oxide at the interfaces [16]. The number of these oxide interfaces and their stability is determined by the kind of catalyst and preparation method (ball-milling), explaining the dependence of the amount of $MgH_{2-\delta}$ on the used catalyst and preparation method.

The sorption kinetics seems to be directly correlated to the amount of $MgH_{2-\delta}$ (Fig. 4). We conclude that destabilized substoichiometric $MgH_{2-\delta}$ plays a keyrole in the fast sorption kinetics observed in these systems. Due to its nearly hysteresis-free hydrogen uptake it can act as a reservoir for the by the catalyst dissociated hydrogen, the gateway through which the

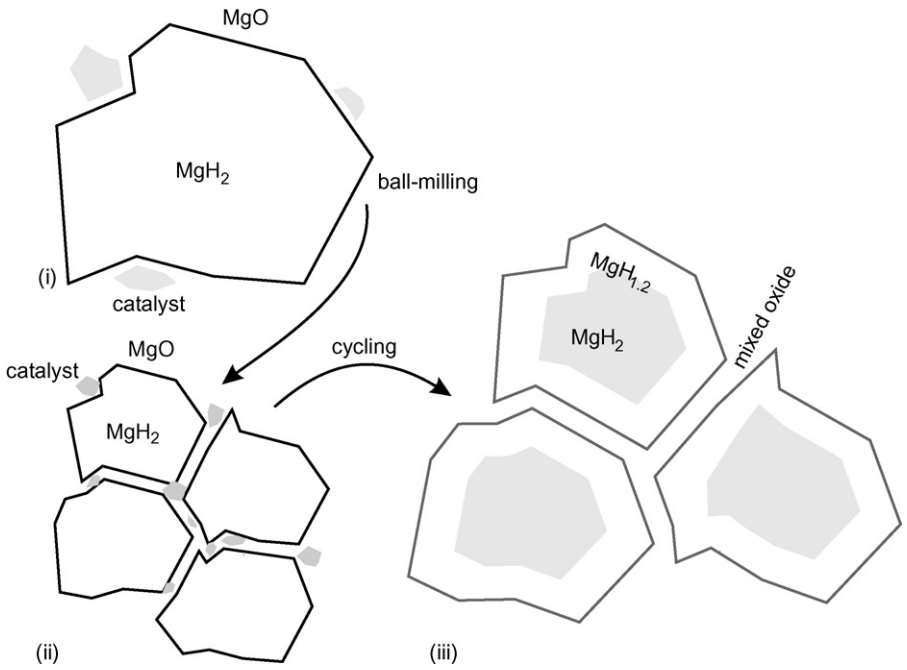

Fig. 9. Depictive model of ball-milled magnesium hydride storage material. (i) MgH_2 powder with catalyst as mixed. (ii) Ball-milled MgH_2 with a crystallite size of less 20 nm. (iii) After cycling the nano-crystallites coarsen. We propose that these clusters consist of a core MgH_2 with a shell of destabilized $MgH_{2-\delta}$ due to oxide interfaces formed with the attached catalysts.

hydrogen enters (diffuses) into the grains. This explains, why oxides are better catalysts than pure 3d-metals [4,5] even though they exhibit a much lower dissociation probability [8], as they increase the amount of the destabilized phase. Supporting dissociation is one required property, an as important one seems to be the ability to form oxide interfaces to destabilize the magnesium hydride phase. Our results are in fair agreement with recently published data on the hydrogenation characteristics of MgH_2 catalyzed with nano-sized Nb_2O_5 [30]. The authors also proposed a 'pathway-model', which explains the kinetic hydrogen sorption improvement by a formation of pathways of niobium oxide species. In contrast to this publication, we have shown here that the catalyst *induces* the pathways (destabilized $MgH_{2-\delta}$) instead of being one. Based on this model, some empirical correlations can be explained. Barkhordarian et al. [32] reported that maximum kinetics is found for oxides with a low stability, which nevertheless has to be high enough to avoid complete reduction of the transition metal under operating conditions. From the above given discussion it is evident that a favorable oxide catalyst chemically interacts with the hydride, while a total oxidation of the Mg is prevented by the high stability of the catalyst. This fits to the observation that kinetics as high as measured in mildly milled Nb_2O_5-catalyzed MgH_2 can also be achieved in MgO-catalyzed MgH_2 after an extremely long ball-milling procedure [33], whereas MgO was found to be less active than Nb_2O_5 under identical preparation conditions. Obviously, the number of oxide interfaces is the important parameter for a fast kinetics. Similarly, it was found that a *small* dose of air improves the desorption kinetics of oxygen-free vanadium-catalyzed MgH_2 [31], probably due to oxygen, which generates oxide interfaces in the material.

5. Conclusions

Catalysts in metal hydrides are the philosopher's stones in hydrogen storage. Their effective activity has been demonstrated for many systems (e.g. oxides in MgH_2, Ti in $NaAlH_4$ [34]), while their functioning is still controversially debated. The simplicity of the Mg–MgH_2 systems predestines it as a model system to study the functioning of such catalysts. Indeed several studies were published, which can be summarized by the general idea that catalysts support dissociation of hydrogen [6] and accelerate the formation of MgH_2 via a spill-over effect [3]. However, this model fails in explaining the higher activity of oxides than that of pure d-metals, as oxides are known to exhibit a much lower dissociation probability for hydrogen. We have shown in this paper by calorimetry and X-ray diffraction that catalysts induce the formation of a destabilized $MgH_{2-\delta}$-phase, which does not exist in unmilled MgH_2. This phase seems to be an additional important ingredient for a fast hydrogen uptake of Mg. In summary: a good additive supports dissociation and destabilizes the hydride. The model is not limited to MgH_2. In particular, similar ideas are discussed for catalysts supporting the formation of $NaAlH_4$: do they support dissociation or do they destabilize the structure [35]? In this paper, we have shown a way to shed light on this question.

Acknowledgement

This work was financially supported by the Helmholtz-Initiative FuncHy.

References

[1] L. Schlapbach, A. Züttel, Nature (London) 414 (2001) 353.
[2] J. Huot, G. Liang, S. Boily, A. Van Neste, R. Schulz, J. Alloys. Compd. 293 (1999) 495.
[3] J.F. Pelletier, J. Huot, M. Sutton, R. Schulz, A.R. Sandy, L.B. Lurio, S.G.J. Mochrie, Phys. Rev. B 63 (2001), 052103.
[4] G. Barkhordarian, T. Klassen, R. Bormann, Scr. Mater. 49 (2003) 213.
[5] N. Hanada, T. Ichikawa, Fujii, J. Phys. Chem. B 109 (2005) 7188.
[6] G. Barkhordarian, T. Klassen, R. Bormann, J. Alloys. Compd. 364 (2004) 242.
[7] R. Hammer, J.K. Norskov, Surf. Sci. 343 (1995) 211;
B. Hammer, J.K. Norskov, Nature 376 (1995) 238.
[8] V.E. Henrich, P.A. Cox, The Surface Science of Metal Oxides, Cambridge University Press, New York, 1994.
[9] A. Borgschulte, R.J. Westerwaal, J.H. Rector, B. Dam, R. Griessen, Appl. Phys. Lett. 85 (2004) 4884.
[10] A. Borgschulte, J.H. Rector, B. Dam, R. Griessen, A. Züttel, J. Catal. 235 (2005) 353.
[11] G. Friedlmeier, M. Groll, J. Alloys. Compd. 253 (1997) 550.
[12] V.P. Zhdanov, A. Krozer, B. Kasemo, Phys. Rev. B 47 (1993), 11044.
[13] J. Renner, H.J. Grabke, Z. Metallkd. 69 (1978) 639.
[14] J. Töpler, H. Buchner, H. Säufferer, K. Knorr, W. Prandl, J. Less-Common Met. 88 (1982) 397.
[15] P. Spatz, A. Aebischer, A. Krozer, L. Schlapbach, Z. Phys. Chem. (Munich) 181 (1993) 955.
[16] H. Gijs Schimmel, J. Huot, L.C. Chapon, F.D. Tichelaar, F.M. Mulder, J. Am. Chem. Soc. 127 (2005) 14348.
[17] L. Schlapbach, Surface properties and activation, in: L. Schlapbach (Ed.), Hydrogen in Intermetallic Compounds II, Springer Verlag, Berlin, 1992.
[18] K. Bohmhammel, B. Christ, G. Wolf, Thermochim. Acta 271 (2005) 67.
[19] K. Bohmhammel, B. Christ, G. Wolf, Thermochim. Acta 310 (1998) 167.
[20] H. Frieske, E. Wicke, Ber. Bunsen-Ges. Phys. Chem. 77 (1973) 50.
[21] J.F. Stampfer, C.E. Holley, J.F. Suttle, J. Am. Chem. Soc. 82 (1960) 3504.
[22] C.X. Shang, M. Bououdina, Y. Song, Z.X. Guo, Int. J. Hydrogen Energy 29 (2004) 73.
[23] W. Oelerich, Sorption properties of nanocrystalline metal hydrides for the storage of hydrogen, thesis, TU Hamburg-Harburg (2000).
[24] P.-A. Huhn, M. Dornheim, T. Klassen, R. Bormann, J. Alloys Compd. 404 (2005) 499–502.
[25] R.W.P. Wagemans, J.H. van Lenthe, P.E. de Jongh, A.J. van Dillen, K.P. de Jong, J. Am. Chem. Soc. 127 (2005) 16675–16680.
[26] A. Miniotas, B. Hjörvasson, L. Douysset, P. Nostell, Appl. Phys. Lett. 76 (2000) 2056.
[27] D. Setoyama, S. Yamanaka, J. Alloys. Compd. 370 (2004) 144.
[28] T.B. Massalski, Binary Alloy Phase Diagrams, ASM International, New York, 1990.
[29] O. Friedrichs, J.C. Sánchez-López, C. López-Cartes, M. Dornheim, T. Klassen, R. Bormann, A. Fernández, Appl. Surf. Sci. 252 (2006) 2334–2345.
[30] O. Friedrichs, J.C. Sanchez-Lopez, C. Lopez-Cartes, M. Dornheim, T. Klassen, R. Bormann, A. Fernandez, J. Phys. Chem. B 110 (2006) 7845.
[31] W. Oelerich, T. Klassen, R. Bormann, J. Alloys Compd. 315 (2001) 237.
[32] G. Barkhordarian, T. Klassen, R.J. Bormann, J. Phys. Chem. B 110 (2006) 11020–11024.
[33] K.-F. Aguey-Zinsou, J.R. Ares Fernandez, T. Klassen, R. Bormann, Mater. Res. Bull. 41 (2006) 1118–1126.
[34] B. Bogdanovic, M. Schwickardi, J. Alloys Compd. 253 (1997) 1.
[35] J. Graetz, J.J. Reilly, J. Johnson, A.Y. Ignatov, T.A. Tyson, Appl. Phys. Lett. 85 (2004) 500.